

Stripe order and magnetic transitions in $\text{La}_{2-x}\text{Sr}_x\text{NiO}_4$ P. G. Freeman,* A. T. Boothroyd, and D. Prabhakaran
*Department of Physics, Oxford University, Oxford OX1 3PU, United Kingdom*M. Enderle
*Institut Laue-Langevin, Boîte Postale 156, 38042, Grenoble Cedex 9, France*C. Niedermayer
Laboratory for Neutron Scattering, ETHZ and PSI, CH-5232 Villigen PSI, Switzerland
(Received 4 March 2004; revised manuscript received 23 April 2004; published 21 July 2004)

Magnetic order has been investigated in stripe-ordered $\text{La}_{2-x}\text{Sr}_x\text{NiO}_4$ ($x=0.275, 0.37, 0.4$) by dc magnetization and by polarized- and unpolarized-neutron diffraction. In the magnetically ordered phase, all three compositions exhibit a magnetic transition consistent with a spin reorientation in the ab plane. For $x=0.37$, the spin axes rotate from an angle of $37.7^\circ \pm 0.3^\circ$ to the stripe direction at 71 K, to $52.3^\circ \pm 0.2^\circ$ at 2 K. The $x=0.275$ and 0.4 compounds were found to undergo a similar spin reorientation. A spin reorientation has now been observed to occur for five different doping levels in the range of $0.275 \leq x \leq 0.5$, suggesting that this spin transition is an intrinsic property of the stripe phase.

DOI: 10.1103/PhysRevB.70.024413

PACS number(s): 75.30.Fv, 71.45.Lr, 75.25.+z

I. INTRODUCTION

$\text{La}_{2-x}\text{Sr}_x\text{CuO}_4$ (LSCO) and $\text{La}_{2-x}\text{Sr}_x\text{NiO}_4$ (LSNO) are isostructural, but it is well known that LSCO superconducts¹ when sufficiently doped, whereas LSNO does not. In LSNO the doped charges are known to localize in the form of charge stripes, i.e., periodically spaced lines of charges at 45° to the Ni-O bonds. Antiferromagnetic ordering of the Ni spins between the charge stripes sets in at lower temperatures.² The charge stripes act as antiphase domain walls to the antiferromagnetic background. The pattern of incommensurate magnetic fluctuations in LSCO³ resembles the magnetic order seen in LSNO, and this has been attributed to the existence of dynamic stripes in LSCO. The fluctuations in superconducting LSCO are centered on wave vectors parallel to the Cu-O bonds,⁴ but the fluctuations in the nonsuperconducting state, $0.024 \leq x \leq 0.053$, are centered on wave vectors at 45° to the Cu-O bonds.⁵ These parallels suggest that charge-stripe correlations may play an important role in superconducting LSCO.⁶

Charge-stripe order has been studied in LSNO by neutron^{2,7-11} and x-ray¹²⁻¹⁴ diffraction for doping levels in the range of $0.135 \leq x \leq 0.5$. As well as being static on the timescale probed by neutrons and x rays, the charge stripes are found to be well correlated with correlation lengths in excess of 100 Å for certain levels of doping.^{2,13,14} These two properties make LSNO a good system for studying the basic properties of spin-charge stripes.

These studies have revealed many key facts about charge-stripe ordering, including the variation of the stability of charge ordering with doping. LSNO with $x=1/3$ has a stripe order that is particularly stable owing to a commensurability effect that pins the charges to the lattice.^{2,9,15} Figure 1(a) shows the commensurate charge ordering that occurs for $x=1/3$. Although this figure shows the charge stripes only residing on the Ni sites, recent tunneling electron microscopy work has shown the charge stripes can also reside on the O

sites.¹⁶ The charge order is even more stable for $x=1/2$, forming a “checkerboard” pattern in the Ni-O₂ layers at temperatures below ~ 480 K, which becomes slightly incommensurate below ~ 180 K.^{10,17}

Lee *et al.*⁸ studied the magnetic order in LSNO crystals with $x=0.275$ and $1/3$ with polarized neutrons in order to determine the direction of the ordered moment. They concluded that at $T=11$ K the spins in the Ni-O₂ layers are aligned at an angle $\pm\phi$ to the stripe direction, where $\phi=27^\circ$ for $x=0.275$ and 52.5° for $x=1/3$. However, for the $x=1/3$ they found a reorientation transition at $T_{\text{SR}} \approx 50$ K

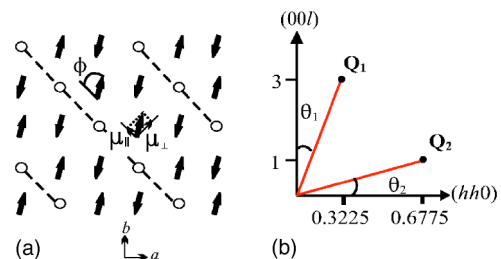


FIG. 1. (Color online) (a) Model for the stripe pattern ordering in the ab plane of $\text{La}_{5/3}\text{Sr}_{1/3}\text{NiO}_4$. Circles represent holes residing on Ni^{3+} sites, while the solid arrows represent the Ni^{2+} spins. Dashed lines indicate the charge domain walls of the stripe order. The occurrence of purely Ni centred stripes may not be realized in practice, especially for $x \neq 1/3$. The observed spin order in $\text{La}_{1.63}\text{Sr}_{0.37}\text{NiO}_{4+\delta}$ is similar to that shown, but is actually incommensurate in the direction perpendicular to the stripes. The components of the ordered moment parallel (μ_{\parallel}) and perpendicular (μ_{\perp}) to the stripe direction are shown, and ϕ denotes the angle between the spin axis and the stripe direction. (b) Diagram of the (h, h, l) plane in reciprocal space. \mathbf{Q}_1 and \mathbf{Q}_2 are the scattering vectors of two magnetic Bragg peaks of the stripe order, chosen to be approximately parallel and perpendicular to the c axis. The particular positions shown in the diagram are those investigated for the case $x=0.37$.

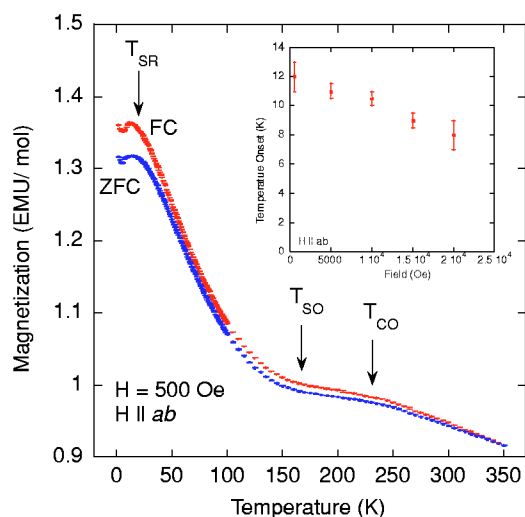


FIG. 2. (Color online) FC and ZFC magnetization data for $\text{La}_{1.63}\text{Sr}_{0.37}\text{NiO}_{4+\delta}$. The arrows indicate the charge-ordering temperature T_{CO} , spin-ordering temperature T_{SO} , and the spin-reorientation temperature T_{SR} , determined separately by neutron diffraction. The inset shows the field dependence of the onset temperature of the anomaly in the magnetization data.

such that on warming, the spins rotate by an angle of $\Delta\phi = 12.5^\circ$ towards the stripe direction. Freeman *et al.*¹¹ studied a sample with $x=1/2$ and observed a similar spin reorientation transition: in this case, at $T=2$ K, $\phi=78^\circ$, $T_{\text{SR}} \approx 57$ K, and $\Delta\phi=26^\circ$.

Although this much is known about the spin orientation in LSNO, the trends have not yet been fully established and the mechanism driving the spin reorientation is not understood. Our study was undertaken to try to address these questions by studying doping levels other than $1/3$ and $1/2$.

We studied single crystals of $\text{La}_{2-x}\text{Sr}_x\text{NiO}_4$ grown by the floating-zone method,¹⁸ using the techniques of magnetometry, ($x=0.275, 0.37, 0.4$), polarized-neutron diffraction ($x=0.37$), and unpolarized-neutron diffraction ($x=0.275, 0.4$). The charge- and magnetic-ordering temperatures were found to be in good agreement with previous work on samples of similar doping.^{2,10} The data reveal a spin reorientation similar in size and orientation to that in $\text{La}_{5/3}\text{Sr}_{1/3}\text{NiO}_4$, but which is slower and occurs at lower temperatures, ~ 15 K, for all three doping levels studied. These spin reorientations, unlike those in the $x=1/2$ or $1/3$ doped materials, all occur for incommensurate doping levels.

II. MAGNETIZATION MEASUREMENTS

Magnetization data were collected with a superconducting quantum interference device (SQUID) magnetometer (Quantum Design), with the field applied parallel to the ab plane of the crystal. The crystals used for the magnetization measurements had typical dimensions $\sim 5 \times 5 \times 2$ mm³. We carried out dc measurements either by cooling the sample in an applied field of 500 Oe parallel to the ab plane (FC), or by cooling in zero field then measuring while warming in a field of 500 Oe (ZFC).

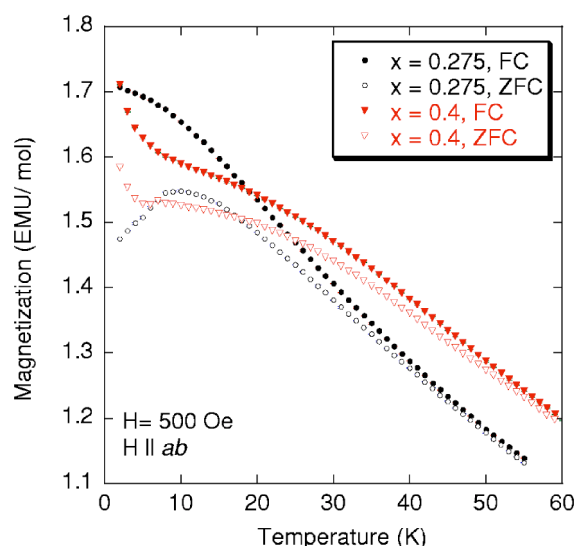


FIG. 3. (Color online) FC and ZFC magnetization data for $\text{La}_{2-x}\text{Sr}_x\text{NiO}_{4+\delta}$ $x=0.275$ and 0.4 .

In Fig. 2 we show the variation of the FC and ZFC magnetizations for $x=0.37$. A subtle change of slope at $T_{\text{CO}} = 230 \pm 10$ K marks the charge-ordering temperature, with a more pronounced gradient change at $T_{\text{SO}} = 170 \pm 10$ K marking the spin-ordering temperature (defined later from neutron diffraction). We observe from these results that this material exhibits irreversible magnetic behavior, with a large FC-ZFC difference below ~ 50 K and a much smaller difference that persists to T_{CO} with a slight widening around T_{SO} . This is a typical feature for magnetization results on LSNO compounds that will be reported in detail elsewhere.¹⁹ Of most concern to the present work is the small but sharp drop in magnetization below ~ 12 K. The inset of Fig. 2 shows the field dependence of this feature, which can be seen to decrease when increasing the applied field. As we will show later, this feature corresponds to a spin reorientation transition.

Figure 3 shows the variation of FC and ZFC magnetizations for the $x=0.275$ and $x=0.4$. Like $x=0.37$, both these materials are observed to have irreversible magnetic behavior. The ZFC magnetization of the $x=0.275$ crystal has a rounded maximum at ~ 10 K. For $x=0.4$ there is no maximum, but the increase in magnetization with decreasing temperature first slows down and then begins to rise sharply below 5 K. The increase below 5 K could be due to a small amount of paramagnetic impurity in the crystal.

III. NEUTRON-DIFFRACTION MEASUREMENTS

The polarized-neutron experiments were performed on the triple-axis spectrometer IN20 at the Institut Laue-Langevin. The energies of the incident and elastically scattered neutrons were selected by Bragg reflection from an array of Heusler alloy crystals. The data were obtained with initial and final neutron wave vectors of 2.66 \AA^{-1} . A pyrolytic graphite (PG) filter was present between the sample and the analyzer to suppress scattering of higher-order harmonics.

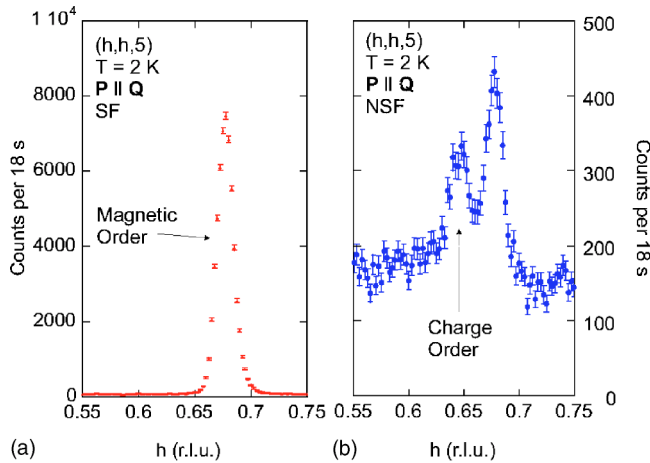


FIG. 4. (Color online) (a) The spin flip (SF) diffraction channel for a scan parallel to $(h, h, 0)$ for $l=5$ for $\text{La}_{1.63}\text{Sr}_{0.37}\text{NiO}_4$ at $T=2$ K. This peak corresponds to the magnetic order peak and is centred at $h=0.678$. (b) The non-spin-flip diffraction for the same scan. The arrow indicates the charge-order Bragg peak. The second peak is diffraction from the magnetic order peak observed in the NSF channel due to the imperfect spin polarization of the neutron beam.

The unpolarized-neutron experiments were performed on the triple-axis spectrometer RITA-II at SINQ at the Paul Scherrer Institut. The energies of the incident and elastically scattered neutrons were selected by Bragg reflection from a PG crystal. The data were obtained with initial and final neutron wave vectors of 1.55 \AA^{-1} , and a Be filter operating at 77 K was present between the sample and the analyzer to suppress scattering of higher-order harmonics.

For $x=0.275, 0.37$, single crystal rods of 7–8 mm diam and ~ 45 mm in length were used, and for $x=0.4$ the crystal was a slab of dimensions $\sim 15 \times 10 \times 4 \text{ mm}^3$. In this work we describe the structural properties of LSNO with reference to a tetragonal unit cell, with unit cell parameters $a \approx 3.8 \text{ \AA}$, $c \approx 12.7 \text{ \AA}$. The samples were mounted with the $[001]$ and $[110]$ crystal directions in the horizontal scattering plane. Scans were performed in reciprocal space either parallel to the $(h, h, 0)$ direction at constant l , or parallel to the $(0, 0, l)$ direction at constant h .

We begin by discussing the polarized-neutron diffraction results for $x=0.37$. Initially, the neutron polarization \mathbf{P} was arranged to be parallel to the scattering vector \mathbf{Q} , by an adjustable guide field of a few mT at the sample position. In this configuration a neutron's spin is flipped during an interaction with electronic magnetic moments, but remains unchanged when scattered by a nonmagnetic process, e.g., a lattice distortion. Thus by measuring the spin-flip (SF) and non-spin-flip (NSF) channels, one can identify whether observed scattering is magnetic in origin or not.

Magnetic order Bragg peaks were observed at $(h + 1/2 \pm \varepsilon/2, h + 1/2 \pm \varepsilon/2, l)$ positions for all integer l . This can be seen in Fig. 4(a), which shows the SF scattering for a scan parallel to $(h, h, 0)$ for $l=5$ at $T=2$ K. The peak positions corresponds to $\varepsilon=0.3554 \pm 0.0002$, consistent with previous measurements.²

Figure 4(b) shows the NSF scattering for the same scan as Fig. 4(a). The scan contains two weak peaks, one at

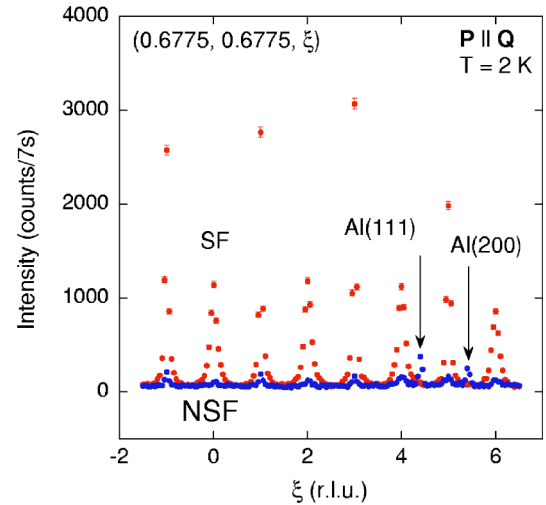


FIG. 5. (Color online) Spin-flip (SF) and non-spin-flip (NSF) diffraction from $\text{La}_{1.63}\text{Sr}_{0.37}\text{NiO}_4$ at $T=2$ K. The scan is parallel to $(0, 0, l)$ and passes through the magnetic-order peak $(0.6775, 0.6775, 1)$. No correction has been made for the imperfect polarization of the neutron beam. The additional peaks in the NSF channel at $l \approx 4.4$ and 5.4 are due to diffraction from the Al sample mount.

$h=0.646 \pm 0.001$ corresponding to charge ordering with an incommensurability of $\varepsilon=0.354 \pm 0.001$, and the other at $h=0.678$ corresponding to magnetic ordering. The latter appears in the NSF channel due to imperfect polarization of the neutron beam. We searched for the charge-order peak at other equivalent $(0.646, 0.646, l)$ positions, but only at $l=3$ and 5 was there a measurable peak. From the temperature dependence of the charge peak in Fig. 4(b) we found $T_{\text{CO}} \approx 230$ K. By performing scans parallel to $(h, h, 0)$ we were able to obtain the in-plane charge-order correlation length perpendicular to the stripe direction of $70 \pm 6 \text{ \AA}$. This compares with a correlation length of $49 \pm 5 \text{ \AA}$ along the c axis. These results show that the charge order is relatively three dimensional.

Figure 5 shows a scan parallel to $(0, 0, l)$ through the magnetic order peaks. The widths of the peaks in this scan relate to the correlation length along the c axis, however we observed that the correlation lengths for even and odd l differ by a factor ≈ 2 . That is, for even l we obtain a correlation length of $53.2 \pm 1.4 \text{ \AA}$ and for odd l we obtain a correlation length of $108 \pm 2 \text{ \AA}$. We performed scans parallel to $(h, h, 0)$ on odd l peaks, for which we obtained an in-plane correlation length perpendicular to a charge stripe direction of $112.6 \pm 1.1 \text{ \AA}$.

The intensities of the even and odd l magnetic peaks were discussed in work on $\text{La}_2\text{NiO}_{4+\delta}$ by Wochner *et al.*²⁰ For a commensurate stripe spin ordering, such as $\varepsilon=1/3$, the stripes stack in a body-centered arrangement and only the odd l magnetic peaks are observed, with the systematic absence of the $l = \text{even}$ peaks. However, for incommensurate spin ordering with the stripes either pinned to the Ni or O sites,¹⁶ perfect body-centered stacking cannot be achieved. The disorder thus created, along with the additional disorder introduced due to differing Coulomb interactions between the ab layers, result in the presence of $l = \text{even}$ peaks. Hence,

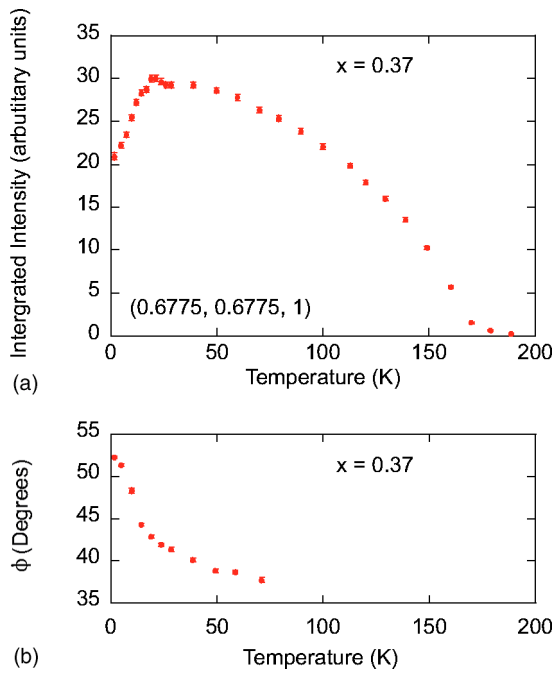


FIG. 6. (Color online) (a) The temperature dependence of the intensity of the magnetic Bragg peak at $\mathbf{Q}_2=(0.6775,0.6775,1)$, [see Fig. 1(b)]. (b) The temperature dependence of the angle ϕ between the spin axis and the stripe direction obtained from polarized-neutron analysis.

$l = \text{odd}$ peaks have a long correlation length as they come from the ideal long range body-centered stacking, whereas $l = \text{even}$ peaks are a result of the disorder created on the smaller length scale of the nonideal stacking.

In Fig. 1(b) are shown the positions of two magnetic reflections, $\mathbf{Q}_1=(0.3225,0.3225,3)$ and $\mathbf{Q}_2=(0.6775,0.6775,1)$. The vectors \mathbf{Q}_1 and \mathbf{Q}_2 are directed close to $(0,0,l)$ and $(h,h,0)$, respectively. Since magnetic neutron diffraction is sensitive to spin components perpendicular to \mathbf{Q} , the scattering at \mathbf{Q}_1 arises mainly from the total in-plane spin moment, while that at \mathbf{Q}_2 comes mainly from the spin components parallel to the stripe direction and along the c axis. Hence, we performed scans parallel to $(h,h,0)$ through \mathbf{Q}_2 at different temperatures to give a first indication as to whether there exists an in-plane spin reorientation like those observed for $x=1/3$ and $1/2$. Figure 6(a) shows the temperature dependence of the magnetic reflection \mathbf{Q}_2 . The magnetic ordering transition can be seen to occur at $T_{SO} \approx 170$ K. On cooling below T_{SO} the intensity of \mathbf{Q}_2 can be seen to increase monotonically until it reaches a maximum at ≈ 20 K, then it is seen to decrease in intensity continuously to our base temperature. This anomalous behavior correlates well with the transition observed in the magnetization, Fig. 2, and indicates a spin reorientation below ≈ 20 K.

To fully analyze the direction of the spins over this temperature range we varied the direction of the neutron polarization \mathbf{P} relative to the scattering vector \mathbf{Q} , measuring at the \mathbf{Q}_1 and \mathbf{Q}_2 positions. The method is described in Ref. 11, where the expressions used to obtain the spin direction are given. A correction for the slightly nonideal performance of the polarization elements of the instrument was calculated

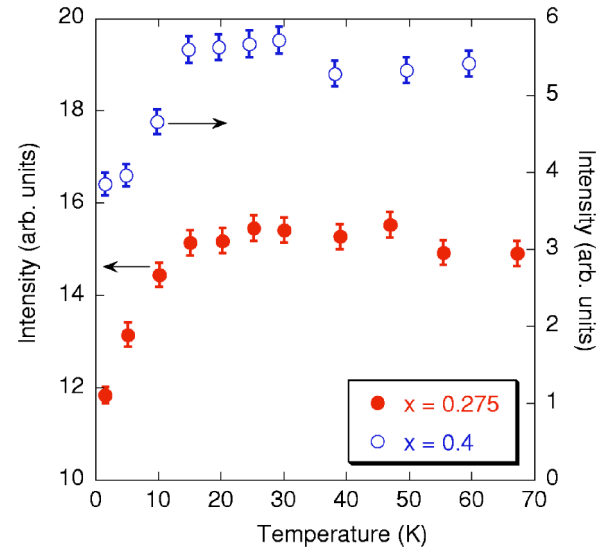


FIG. 7. (Color online) The temperature dependence of the intensity of the magnetic Bragg peak at $\mathbf{Q}_2=(0.645,0.645,0)$ for $x=0.275$, and at $\mathbf{Q}_2=(0.685,0.685,1)$ for $x=0.4$.

from the flipping ratio of 18 ± 1 measured on the magnetic Bragg peaks.

Polarization analysis of both the \mathbf{Q}_1 and the \mathbf{Q}_2 Bragg peaks revealed that the moment lies in the ab plane to within 1° in the temperature range of 2–71 K. Having established this, we subsequently assumed the c -axis component to be zero and analyzed the polarization at \mathbf{Q}_1 to determine the in-plane moment. From this analysis we determined that the spins rotated from an angle of $37.7^\circ \pm 0.3^\circ$ to the stripe direction at $T=71$ K to $52.3^\circ \pm 0.2^\circ$ at $T=2$ K, as shown in Fig. 6(b). The transition occurs mainly between 10 and 20 K, but slowly develops from below ~ 50 K.

We performed unpolarized-neutron diffraction at equivalent \mathbf{Q}_1 and \mathbf{Q}_2 positions on the single crystals with $x=0.275$ and $x=0.4$, using the instrument RITA-II at SINQ. We found a similar behavior to the $x=0.37$ results just described. In particular, the temperature dependence of the $\mathbf{Q}_2=(0.645,0.645,0)$ magnetic Bragg peak for $x=0.275$, and of the $\mathbf{Q}_2=(0.685,0.685,1)$ magnetic Bragg peak for $x=0.4$, both have a maximum similar to that shown in Fig. 6(a) for $x=0.37$. By contrast, the intensities of the \mathbf{Q}_1 Bragg peaks are almost constant below 20 K. The temperature dependence of the \mathbf{Q}_2 intensity is shown in Fig. 7 for both $x=0.275$ and $x=0.4$. The drop in \mathbf{Q}_2 intensity at low temperature implies a spin reorientation in $x=0.4$ and $x=0.275$ similar in nature to that in $x=0.37$.

Unpolarized-neutron diffraction cannot accurately determine ϕ without a detailed analysis of the intensities of many diffraction peaks, but we can estimate $\Delta\phi$ from the drop in intensity of the \mathbf{Q}_2 peak below $T_{SR} \sim 15$ K and the value of ϕ for $T > T_{SR}$, assuming the ordered moment remains in the ab plane and fixed in magnitude in this temperature range. Taking $\phi=27^\circ$ above T_{SR} for $x=0.275$,⁸ and using $\phi=38^\circ$ for $x=0.4$ (based on the observations for $x=0.37$ at 71 K), we find $\Delta\phi \approx 10^\circ - 15^\circ$ for both $x=0.275$ and $x=0.4$, similar to $x=0.37$.

TABLE I. A summary of the characteristic ordering parameters of $\text{La}_{2-x}\text{Sr}_x\text{NiO}_4$.

x	T_{CO} (K)	T_{SO} (K)	ε	T_{SR} (K)	$\phi(2\text{ K})$ (deg)	$\Delta\phi$ (deg)
0.275	$160 \pm 10^{\text{a}}$	130 ± 10	0.296 ± 0.001	12.5 ± 2.5	41 ± 8	10–15
0.333 ^b	240 ± 5	200 ± 5	0.333 ± 0.001	50 ± 5	53 ± 2.5	13 ± 4
0.37	230 ± 10	170 ± 5	0.354 ± 0.001	19 ± 1.5	52.3 ± 0.2	14.6 ± 0.4
0.4	$180 \pm 20^{\text{c}}$	150 ± 10	0.371 ± 0.001	15 ± 2.5	–	10–15
0.5	$480 \pm 30^{\text{c}}$	80 ± 10	0.443 ± 0.001	57 ± 2	78 ± 3	26 ± 5

^aData taken from Ref. 14.^bData taken from Ref. 8.^cData taken from Ref. 10.

IV. DISCUSSION AND CONCLUSIONS

To aid the discussion of our results we refer to Table I, which summarizes the ordering values for each doping level. There are differences and similarities between the spin reorientations reported here for $x=0.275$, 0.37, and 0.4 and those that occur for $x=1/3$,⁸ and $x=1/2$.¹¹ In each case the spins rotate in the same sense, away from the stripe direction on cooling. The size of the reorientation in $x=0.37$ ($\Delta\phi \approx 14.6^\circ$), and more approximately in $x=0.275$ and 0.4, is similar to that in $x=1/3$ ($\Delta\phi \approx 13^\circ$), but smaller than in $x=1/2$ ($\Delta\phi \approx 26^\circ$). However, in $x=0.37, 0.275$, and 0.4 the spin reorientation occurs at a much lower temperature, $T_{\text{SR}} \approx 15\text{ K}$, compared with $T_{\text{SR}} \approx 50\text{ K}$ for $x=1/3$ and $T_{\text{SR}} \approx 57\text{ K}$ for $x=1/2$. Figure 8 summarizes the variation of T_{SR} with x that has so far been established for the doping range

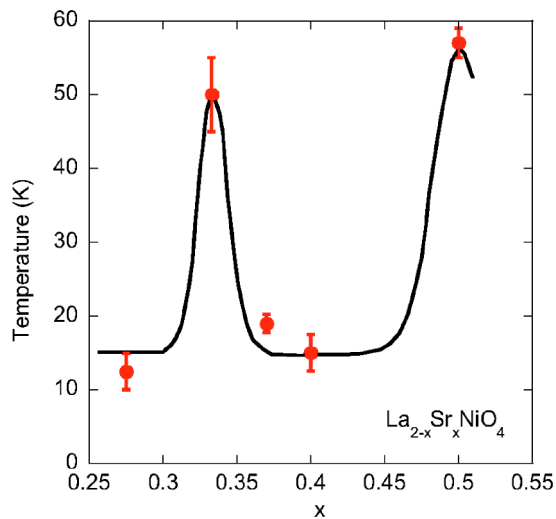


FIG. 8. (Color online) Variation with doping level x of the spin-reorientation temperature T_{SR} , defined as the temperature at which the \mathbf{Q}_2 Bragg peak starts to lose intensity on cooling. The line is a guide to the eye indicating the possible trend. The value for $x=1/3$ is taken from Ref. 8.

of $0.275 \leq x \leq 0.5$. The results indicate that for general doping levels the spin reorientation occurs around 15 K, but the particular compositions $x=1/3$ and $x=1/2$ are exceptional in having $T_{\text{SR}} \approx 50\text{ K}$.

There is also evidence of a trend in the direction of the ordered moment. The base temperature spin orientations are 53° for $x=1/3$, 52° for $x=0.37$, and 78° for $x=1/2$, with charge-ordering temperatures of ~ 240 , ~ 230 , $\sim 480\text{ K}$, respectively. We can add to this list an estimate of $41 \pm 8^\circ$ for $x=0.275$, (charge-ordering temperature $\sim 160\text{ K}$) based on the angle of $27 \pm 7^\circ$ at 11 K found by Lee *et al.*,⁸ with an additional $10^\circ - 15^\circ$ due to the spin reorientation on cooling to 2 K. Hence, there seems to be a correlation between the spin-orientation angle ϕ and the charge-ordering temperature. Further measurements on samples with doping levels between $x=0.4$ and 0.5 would be useful to confirm this trend.

Up to now, spin reorientations in $\text{La}_{2-x}\text{Sr}_x\text{NiO}_4$ had only been observed in materials with an especially stable charge order ($x=1/3$ and $1/2$). The existence of a spin reorientation in $x=1/2$ has shown that a commensurate spin-stripe order is not required for a spin reorientation to occur.¹¹ The results on $x=0.275$, 0.37, and 0.4 presented here further show that not even commensurate doping is required. It is likely that LSNO at all doping levels in the range of $0.275 \leq x \leq 0.5$ undergo a spin reorientation, but that T_{SR} is larger at the commensurate doping compositions.

We are unaware of any model that explains the spin reorientation in $\text{La}_{2-x}\text{Sr}_x\text{NiO}_4$. Such a model needs to predict the three important properties we have identified in this work; (i) that the spin reorientation occurs for all doping levels in the range of $0.275 \leq x \leq 0.5$, (ii) that T_{SR} is particularly high in the $x=1/3$ and $x=1/2$ compounds, and (iii) that the spin reorientation can be suppressed by application of magnetic field.

This work was supported in part by the Engineering and Physical Sciences Research Council of Great Britain. Some of this work was performed at the Swiss Spallation Neutron Source SINQ, Paul Scherrer Institute (PSI), Villigen, Switzerland.

*URL: <http://xray.physics.ox.ac.uk.Boothroyd>

- ¹J. G. Bednorz and K. A. Müller, *Z. Phys. B: Condens. Matter* **64**, 189 (1986).
- ²H. Yoshizawa, T. Kakeshita, R. Kajimoto, T. Tanabe, T. Katsufuji, and Y. Tokura, *Phys. Rev. B* **61**, R854 (2000).
- ³T. R. Thurston, R. J. Birgeneau, M. A. Kastner, N. W. Preyer, G. Shirane, Y. Fujii, K. Yamada, Y. Endoh, K. Kakurai, M. Matsuda, Y. Hidaka, and T. Murakami, *Phys. Rev. B* **40**, 4585 (1989); S-W. Cheong, G. Aeppli, T. E. Mason, H. Mook, S. M. Hayden, P. C. Canfield, Z. Fisk, K. N. Clausen, and J. L. Martinez, *Phys. Rev. Lett.* **67**, 1791 (1991); T. E. Mason, G. Aeppli, and H. A. Mook, *ibid.* **68**, 1414 (1992); T. R. Thurston, P. M. Gehring, G. Shirane, R. J. Birgeneau, M. A. Kastner, Y. Endoh, M. Matsuda, K. Yamada, H. Kojima, and I. Tanaka, *Phys. Rev. B* **46**, 9128 (1992).
- ⁴K. Yamada, C. H. Lee, K. Kurahashi, J. Wada, S. Wakimoto, S. Ueki, H. Kimura, Y. Endoh, S. Hosoya, G. Shirane, R. J. Birgeneau, M. Greven, M. A. Kastner, and Y. J. Kim, *Phys. Rev. B* **57**, 6165 (1998).
- ⁵S. Wakimoto, G. Shirane, Y. Endoh, K. Hirota, S. Ueki, K. Yamada, R. J. Birgeneau, M. A. Kastner, Y. S. Lee, P. M. Gehring, and S. H. Lee, *Phys. Rev. B* **60**, R769 (1999); S. Wakimoto, R. J. Birgeneau, M. A. Kastner, Y. S. Lee, R. Erwin, P. M. Gehring, S. H. Lee, M. Fujita, K. Yamada, Y. Endoh, K. Hirota, and G. Shirane, *ibid.* **61**, 3699 (2000); M. Matsuda, M. Fujita, K. Yamada, R. J. Birgeneau, M. A. Kastner, H. Hiraka, Y. Endoh, S. Wakimoto, and G. Shirane, *ibid.* **62**, 9148 (2000); M. Fujita, K. Yamada, H. Hiraka, P. M. Gehring, S. H. Lee, S. Wakimoto, and G. Shirane, *ibid.* **65**, 064505 (2002).
- ⁶J. M. Tranquada, B. J. Sternlieb, J. D. Axe, Y. Mkaamura, and S. Uchida, *Nature (London)* **375**, 561 (1995).
- ⁷S. M. Hayden, G. H. Lander, J. Zarestky, P. J. Brown, C. Stassis, P. Metcalf, and J. M. Honig, *Phys. Rev. Lett.* **68**, 1061 (1992); V. Sachan, D. J. Buttrey, J. M. Tranquada, J. E. Lorenzo, and G. Shirane, *Phys. Rev. B* **51**, 12 742 (1995); J. M. Tranquada, D. J. Buttrey, and V. Sachan, *Phys. Rev. B* **54**, 12 318 (1996).
- ⁸S.-H. Lee, S.-W. Cheong, K. Yamada, and C. F. Majkrzak, *Phys. Rev. B* **63**, 060405 (2001).
- ⁹R. Kajimoto, T. Kakeshita, H. Yoshizawa, T. Tanabe, T. Katsufuji, and Y. Tokura, *Phys. Rev. B* **64**, 144432 (2001).
- ¹⁰R. Kajimoto, K. Ishizaka, H. Yoshizawa, and Y. Tokura, *Phys. Rev. B* **67**, 014511 (2003).
- ¹¹P. G. Freeman, A. T. Boothroyd, D. Prabhakaran, D. González, and M. Enderle, *Phys. Rev. B* **66**, 212405 (2002).
- ¹²E. D. Isaacs, G. Aeppli, P. Zschack, S-W. Cheong, H. Williams, D. J. Buttrey *et al.*, *Phys. Rev. Lett.* **72**, 3421 (1994); A. Vigliante, M. von Zimmermann, J. R. Schneider, T. Frello, N. H. Andersen, J. Madsen, D. J. Buttrey, Doon Gibbs, and J. M. Tranquada, *Phys. Rev. B* **56**, 8248 (1997).
- ¹³Yu. G. Pashkevich, V. A. Blinkin, V. P. Gnezdilov, V. V. Tsapenko, V. V. Eremanko, P. Lemmens, M. Fischer, M. Grove, G. Guntherodt, L. Degiorgi, P. Wachter, J. M. Tranquada, and D. J. Buttrey, *Phys. Rev. Lett.* **84**, 3919 (2000).
- ¹⁴P. D. Hatton, M. E. Ghazi, S. B. Wilkins, P. D. Spencer, D. Mannix, T. d'Almeida, D. Prabhakaran, A. T. Boothroyd, and S-W. Cheong, *Physica B* **318**, 289 (2002).
- ¹⁵A. P. Ramirez, P. L. Gammel, S-W. Cheong, D. J. Bishop, and P. Chandra, *Phys. Rev. Lett.* **76**, 447 (1996).
- ¹⁶Jianqi Li, Yimei Zhu, J. M. Tranquada, K. Yamada, and D. J. Buttrey, *Phys. Rev. B* **67**, 012404 (2003).
- ¹⁷C. H. Chen, S-W. Cheong, and A. S. Cooper, *Phys. Rev. Lett.* **71**, 2461 (1993).
- ¹⁸D. Prabhakaran, P. Isla, and A. T. Boothroyd, *J. Cryst. Growth* **237**, 815 (2002).
- ¹⁹P. G. Freeman, A. T. Boothroyd, D. Prabhakaran, and D. González, *J. Magn. Magn. Mater.* **272-276**, Part 1, 265 (2004); P. G. Freeman, A. T. Boothroyd, and D. Prabhakaran (unpublished).
- ²⁰P. Wochner, J. M. Tranquada, D. J. Buttrey, and V. Sachan, *Phys. Rev. B* **57**, 1066 (1998).